

# Identification of Electron Donor States in N-doped Carbon Nanotubes

R. Czerw<sup>1</sup>, M. Terrones<sup>2,3</sup>, J.-C. Charlier<sup>4</sup>, X. Blase<sup>5</sup>, B. Foley<sup>1,6</sup>, R. Kamalakaran<sup>2</sup>, N. Grobert<sup>7</sup>, H. Terrones<sup>3</sup>,  
P. M. Ajayan<sup>8</sup>, W. Blau<sup>6</sup>, D. Tekleab<sup>1</sup>, M. Rühle<sup>2</sup>, and D. L. Carroll<sup>1</sup>

<sup>1</sup>*Dept. of Physics and Astronomy, Clemson University, Clemson SC 29634, USA*

<sup>2</sup>*Max-Planck-Institut für Metallforschung, Seestrasse 92, D-70174 Stuttgart, Germany*

<sup>3</sup>*Instituto de Física, Laboratorio Juriquilla, UNAM, A.P. 1-1010, 76000, Querétaro, México*

<sup>4</sup>*Unité de Physico-Chimie et de Physique de Matériaux, Université Catholique de Louvain, Place Croix du Sud 1, B-1348, Louvain-la-Neuve, Belgium*

<sup>5</sup>*Département de Physique des Matériaux, Université Claude Bernard, 43 bd. du 11 Novembre 1918, 69622 Villeurbanne Cedex, France*

<sup>6</sup>*Dept. of Physics, Trinity College Dublin, Dublin 2, Ireland*

<sup>7</sup>*Fullerene Science Center, CPES, University of Sussex, Brighton BN1 9 QJ, UK*

<sup>8</sup>*Dept of Materials Science and Engineering, Rensselaer Polytechnic Institute, Troy NY 12180-3590, USA*  
(September 25, 2018)

Nitrogen doped carbon nanotubes have been synthesized using pyrolysis and characterized by Scanning Tunneling Spectroscopy and transmission electron microscopy. The doped nanotubes are all metallic and exhibit strong electron donor states near the Fermi level. Using tight-binding and *ab initio* calculations, we observe that pyridine-like N structures are responsible for the metallic behavior and the prominent features near the Fermi level. These electron rich structures are the first example of n-type nanotubes, which could pave the way to real molecular hetero-junction devices.

PACS numbers: 61.46.+w, 81.07.De, 68.37.Ef

Carbon nanotubes hold enormous promise in a wide variety of electronic applications including, nano-heterojunctions [1–3], diodes [4], interconnects [5–7], nano-transistors [8,9], sensors [10,11], etc. The addition of dopants (e.g. N or B) within the lattice of carbon nanotubes has suggested that such applications might be realized. In this context, it has been shown that B-doping of multiwalled carbon nanotubes (MWNTs) results in the addition of acceptor states near the valence band edge [12,13]. Further examples, such as doping through ‘topological’ defects, result in the introduction of electronic defect states (e.g. by incorporating 5/7 defects via Stone-Wales type transformations) [14,15]. These ‘dopants’ have also been theoretically predicted to result in acceptor and donor states near the Fermi level [16]. Although the exact mechanisms and lattice effects of such doping schemes in carbon nanotubes differ slightly to those of bulk materials such as Si, the similarities to semiconductor physics are striking. However, the majority of the predicted and all of the experimentally studied dopant effects result in modifications to the valence band, and consequently the p-type conduction in carbon nanotubes. This may be generally due to the nature of the  $sp^2$ -bonded graphene lattice. Electron rich substitutions in such lattices could easily lead to ‘out of plane’ bonding configurations, which may induce curvature and closure of the system during growth before tubular formation occurs. For a complete analogy to bulk semiconductor technology in low dimensional materials, we must seek to dope the materials such that n-type and

p-type conduction occurs. Therefore, it is necessary to introduce donor states to the system as well as acceptor states.

In this study we demonstrate that N-doping of the carbon nanotube lattice, produced by pyrolytic routes, results in the substitutional introduction of N into the C network. From tunneling spectroscopy studies, it is clear that the electronic structure of these doped nanotubes was strongly modified by including electron donor states near the conduction band edge. The identification of the lattice ‘defects’ was carried out by tunneling spectroscopy and confirmed theoretically using tight binding and *ab initio* calculations by comparing the calculated local density of states (LDOS) with that obtained experimentally. The results indicate that pyridine-like N (two-bonded N) units embedded within the nanotube carbon lattice, which differs from the direct substitution of three-fold coordinated carbon, is responsible for a strong DOS in the conduction band close to the  $E_f$ .

Multiwalled  $CN_x$  carbon nanotubes/nanofibres were synthesized by pyrolyzing ferrocene/melamine mixtures at 1050 °C in an Ar atmosphere. This technique has been recently described [17,18]. The produced material consists of carpet-like structures containing highly oriented nanotubes/nanofibres of uniform diameter and length. HRTEM studies (JEM4000 EX operating at 400 keV) of the products reveal the presence of nanofibres exhibiting ‘bamboo-like’ units, in which long and straight segments (100-500 nm) of crystalline MWNTs are connected by relatively ‘disordered’ material.

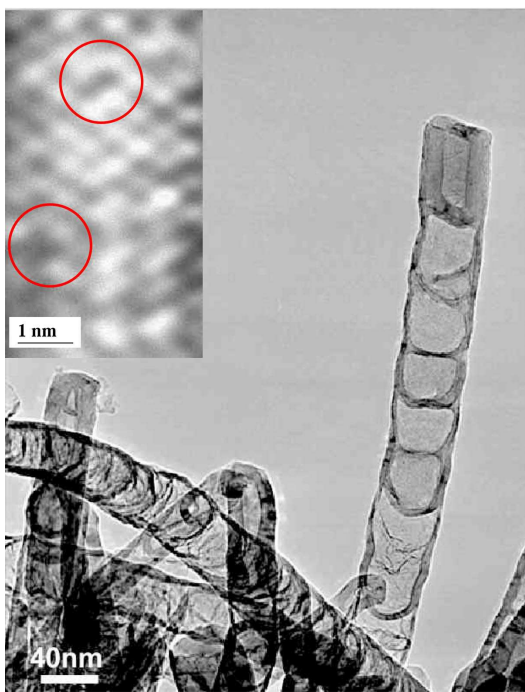


FIG. 1. TEM image of typical N-doped fibers produced by pyrolysis. Note the ‘bamboo-like’ structure consisting of interconnected short (50-100 nm long) and hollow nanotube segments. (inset) Atomic resolution STM image of a small area on the surface of a 20 nm diameter nanotube exhibiting distortions and holes as discussed in the text.

These ‘bamboo-type’ structures are observed in Fig. 1 (TEM and STM-inset). The walls of the ‘bamboo’ segments exhibit some disorder or distortion on the atomic scale (Fig. 1-inset). It is noteworthy that the straight sections of the nanotube appear crystalline in TEM with only small distortions along the outer layers, while in STM large holes or gaps in the lattice are clearly evident (circled region in Fig. 1-inset). As will be seen later, we attribute such holes to lattice discontinuities with nitrogen decoration. High resolution electron energy loss spectroscopy (HREELS) studies of these and similar materials reveal the incorporation of N within the graphene lattice at levels between 2 % and 10 % (atom percent) [17–21].

For the STM study, flakes of the aligned carbon nanotubes/nanofibres were dispersed ultrasonically in tetrahydrofuran (THF). Exceptionally long ultrasonication was necessary to breakup the tube bundles. However, TEM revealed little (if any) damage resulting from this treatment. This solution was then drop cast onto freshly cleaved highly oriented pyrolytic graphite (HOPG). All STM was performed under ultra high vacuum conditions ( $< 10^{-9}$  Torr) using mechanically formed Pt - Ir tips. Stable imaging of the tubes was possible over an STM setpoint range of  $\pm 500$  mV @ 20 - 500 pA. Lattice images of HOPG were used for X-Y calibration of the instrument while the step height of Au was used

for Z-calibrations. Images and spectra were acquired at room temperature. STS was carried out concurrently with image acquisition to insure tip placement on the tube structure. All STS was performed between  $\pm 1.5$  V to prevent serious distortions or damage to the tube at higher voltages and currents. The spectra were acquired at a fixed gap distance for a variety of setpoints.

Fig. 2 compares several tunneling spectra taken along a straight section of the N-doped nanotube (Fig. 2a) with those of a standard (pure) multiwalled carbon nanotube (MWNT) (Fig. 2b). All spectra were converted to the equivalent local density of electronic states (LDOS) using the accepted Feenstra algorithm of numerical differentiation and normalization for tip height:  $(dI/dV)/(I/V)$ . It is important to note that all spectra analyzed in this work were taken from areas over nanotubes that could be identified as clean and free from ‘carbonaceous’ and distorted surroundings. For statistical completeness, several hundreds of spectra from ten different tubes were recorded and compared. The spectra shown here are representative of this sampling and are for tubes that exhibit similar outer shell diameter (ca. 20 nm). Notice that the valence and conduction band features in the pure carbon tube (Fig. 2b) appear symmetric about the Fermi level, while for the N-doped tube (Fig. 2a) an additional electronic feature occurs at  $\sim 0.18$  eV. We also note that the presence of an electronic density of states (DOS) at the  $E_f$  indicates that the N-doped material is metallic. In addition, the electronic structure away from the Fermi level is typical for MWNT’s, exhibiting a variety of symmetric features about the Fermi level (0 eV) that arise from the one-dimensional nature of the nanotube and its inner shells. The electron donor feature seen in the N-doped material is seen everywhere along the straight sections of the nanotubes. The several spectra shown in Fig. 2 are taken on the same section but at different locations, and they exhibit the N-doping feature consistently at the same energy. This result is in contrast to the B-doped case [12], where variations in the peak position are observed due to the formation of local phases, suggesting that the N is distributed along the nanotube with small variations in the N concentration (also observed experimentally in Ref. 18) but no segregation into a separate phase.

There are several ways in which N can be incorporated in the nanotube lattice [22,23]. Earlier theoretical studies [24] have predicted donor states related to N-dopants within carbon nanotubes at 0.27 eV below the bottom of the conduction bands. However, these calculations were performed for large band gap semiconducting single walled nanotubes (chiral and small diameter tubes) and are not directly applicable here. Another previous theoretical investigation [16] demonstrates that N placed substitutionally and fully coordinated into the carbon lattice of a (10,10) single walled tube results in quasibound electronic states approximately 0.53 eV from the Fermi level.

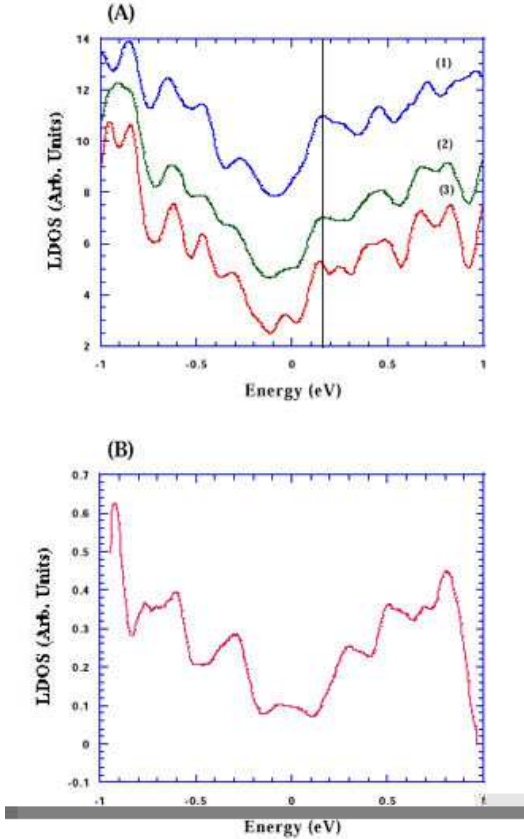


FIG. 2. (a) Tunneling spectra acquired on a straight section of an N-doped carbon nanotube. Spectra (1) - (3) were taken at different locations along the surface but close to a hole as shown in Fig. 1-inset. Note the peak at 0.18 eV in all spectra. (b) Tunneling spectra along a pure MWNT of 20 nm. Notice the regularly spaced van Hove singularities signifying the one-dimensional nature of the material.

In the present study, we have performed *ab initio* band structure calculations of N-doped graphitic systems, within the local density approximation of density functional theory, in order to simulate more accurately the doping effect on larger tube surfaces [25] as measured here. A 3x3 graphite unit cell was adopted, in which one of the 18 C atoms was replaced by a N atom, leading to a  $\sim 5.5\%$  substitutional doping. The main effect of the N dopant in the ‘graphitic’ DOS is the raising of the Fermi level by  $\sim 1.21$  eV. There are indeed N-states close-above the Fermi energy (in agreement with Ref. [16]). On general grounds, one may expect that the exact location of these states will depend on doping level and local curvature of the graphene sheet. However, these donor states, related to an isolated N atom, are completely delocalized over several Angstroms due to the metallic character of the undoped host structure, and they are unable to explain the strong donor peak observed experimentally in Fig. 2.

Careful experimental examination of the  $N-\pi^*$  edge in

HREELS reveals the formation of pyridine-type ( $sp^2$ -like) structures within the lattice [19]. Therefore, an alternative model for N-incorporation into the lattice might be seen as that shown in Fig. 3 in which N rich cavities are formed throughout the predominately ‘graphitic’ network. Further evidence for such a model is observed in STM (Fig. 1-inset), which reveals lattice ‘holes’ and local atomic distortions along the tube. We observe that STM imaging of these materials proves to be extraordinarily challenging as compared to pure MWNTs due to the presence of local instabilities and lattice distortions.

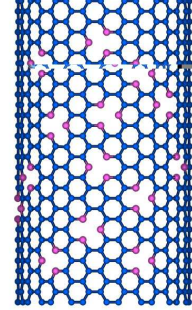


FIG. 3. Random N-doped (15,15) carbon nanotube with a pyridine-like structure: The N is bonded to two carbon atoms (N: red Spheres, C: blue spheres)

In fact, the model consisting of pyridine-like units included in carbon tubules results in a different electronic behavior from those considered theoretically. Specifically, the origin of the low energy electronic states can be observed using tight binding electronic structure calculations of the atomic arrangement as shown in Fig. 3. A simple recursion approach [26], which has proved to capture the essential features associated with composite  $B_xC_yN_z$  nanotube heterojunctions [1], is used to investigate the local DOS associated with the N dopants arranged randomly and homogeneously in a pyridine-like configuration within armchair and zigzag carbon nanotubes [27]. Both DOS, represented in Fig. 4, exhibit prominent donor peaks close-above the Fermi energy, in good agreement with the experimentally determined peak positions of the N-doped tubes (Fig. 2). As a consequence, N doping using pyridine-type units is responsible for a strong related  $\pi$  peak (shown in black, Fig. 4) just above the Fermi energy of the original undoped carbon nanotube (red curves, Fig. 4). It is noteworthy that it does not clearly result in an increase of the Fermi level of the host carbon nanotube as in the case of an isolated N substituted in graphite.

For SWNT’s, the dopant states are quasibound states, which are 1-D analogues of n-type donors in semiconductors. Since these states are resonant with the continuum of conducting states in the 1-D case, the local conductance of the tube near the defect area drops [16]. In the N-doped MWNT case, the observed ‘bamboo’ structure

will almost certainly be the dominate scattering mechanism in the tube. Tunneling spectroscopy over regions that could be clearly identified as interconnections between the nanotube sections show that these regions are also highly conductive (not shown).

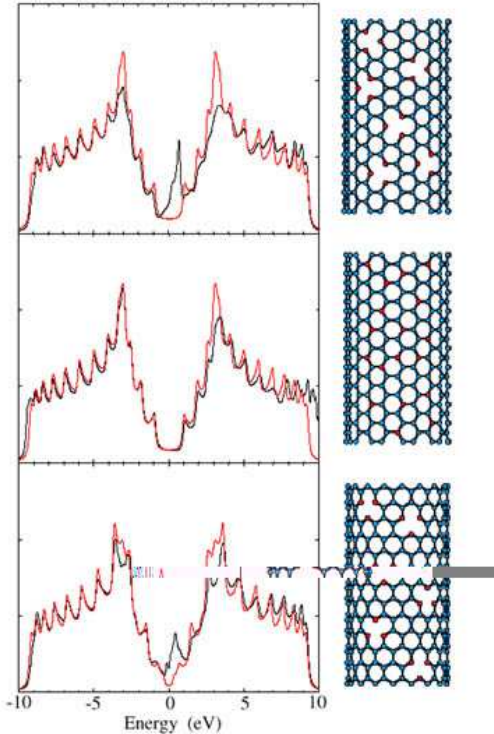


FIG. 4. Theoretical LDOS associated with a Pyridine-like structure of N-doping in (top) armchair (10,10) and (bottom) zigzag (17,0) nanotubes. In both cases, a random, but homogeneous doping (N: red spheres - C: blue spheres) is adopted as illustrated on the right-hand side of the figure. The LDOS of doped (black curve) and pure (red curve) carbon nanotubes are compared. Such Pyridine-like structure of N-doping is responsible for the prominent donor-like features close-above the Fermi energy. Note that the semiconducting (zigzag) nanotube becomes metallic after introducing N in the carbon lattice.

The results presented here also provide the first evidence of the synthesis of local domains of the predicted planar  $C_3N_4$  or CN [22,28,29] within MWNT's (exhibiting the topology of our pyridine-like structures). However, our CNx structures are not crystalline in three dimensions and appear to be discontinuous along the tube surface, which may also explain the fact that all tubular structures are metallic. However, the mechanical properties of these tubes may be important in the fabrication of composites of high tensile strength [23] and shock absorbers.

In summary, we have demonstrated that N-doping of

carbon nanotubes leads to the introduction of conduction band modifications including a large electron donor state. This narrow state lies approximately 0.2 eV from the Fermi level. The local environment of the N within the carbon network mainly consists of N-C structures arranged in a pyridine-like configuration, which also explains the metallic behavior observed in these nanostructures. Our calculations reveal that electronic signatures of pyridine-like units are relatively insensitive to tube chirality or the proximity between these rings. This novel doping scheme not only supplies us with a road map for insertion of other electron rich impurities in the carbon lattice for the creation of donor states but may well suggest a way to achieve full p-n junctions in carbon nanotubes. Interestingly, we note that connections between B-doped carbon nanotubes reported elsewhere [12,13,30] and these materials should result in a barrier of approximately 0.5 V.

We are grateful to AFOSR (DLC), the NSF (DLC), the Alexander von Humboldt Stiftung (MT), CONACYT-México grants: 25237 and J31192U (HT, MT), DGAPA-UNAM grant 108199 (HT), the Royal Society (NG) and the Max-Planck-Gesellschaft (RK). JCC acknowledges the National Fund for Scientific Research [FNRS] of Belgium and the Belgian Program on Inter-university Attraction Poles on Reduced Dimensionality Systems (PAI4/10). Part of this work is carried out within the framework of the EU COMELCAN contract (HPRN-CT-2000-00128). PMA acknowledges the National Science Foundation for supporting his research through the CAREER program.

- 
- [1] X. Blase, J.C. Charlier, A. DeVita, and R. Car, Appl. Phys. Lett. **70**, 197 (1997).
  - [2] J.T. Hu, O.Y. Min, P.D. Yang, and C.M. Lieber, Nature (London) **399**, 48 (1999).
  - [3] Y. Zhang, T. Ichihashi, E. Landree, F. Nihey, and S. Iijima, Science **285**, 1719 (1999).
  - [4] R.D. Antonov, and A.T. Johnson, Phys. Rev. Lett. **83**, 3274 (1999).
  - [5] Y. Y. Wei and G. Eres, Appl. Phys. Lett. **76**, 3759 (2000).
  - [6] M. Terrones, H. Terrones, J.C. Charlier, F. Banhart, and P.M. Ajayan, Science **288**, 1226 (2000).
  - [7] M.S. Fuhrer *et al.*, Science **288**, 494 (2000).
  - [8] S.J. Tans, A.R.M. Verschueren, and C. Dekker, Nature (London) **393**, 49 (1998).
  - [9] S.J. Tans and C. Dekker, Nature (London) **404**, 834 (2000).
  - [10] J. Kong *et al.*, Science **287**, 622 (2000).
  - [11] P.G. Collins, K. Bradley, M. Ishigami, and A. Zettl, Science **287**, 1801 (2000).
  - [12] D.L. Carroll *et al.*, Phys. Rev. Lett. **81**, 2332 (1998).
  - [13] X. Blase *et al.*, Phys. Rev. Lett. **83**, 5078 (1999).

- [14] V.H. Crespi, M.L. Cohen, and A. Rubio, Phys. Rev. Lett. **79**, 2093 (1997).
- [15] H. Terrones, M. Terrones, E. Hernández, N. Grobert, J.C. Charlier, and P. M. Ajayan, Phys. Rev. Lett. **84**, 1716 (2000).
- [16] H.J. Choi, J. Ihm, S.G. Louie, and M.L. Cohen, Phys. Rev. Lett. **84**, 2917 (2000).
- [17] M. Terrones et al., Appl. Phys. Lett. **75**, 3932 (1999).
- [18] W.Q. Han et al., Appl. Phys. Lett. **77**, 1807 (2000).
- [19] M. Terrones et al., Adv. Mater. **11**, 655 (1999).
- [20] M. Terrones et al., Chem. Phys. Letts. **285**, 299 (1998).
- [21] B.C. Satishkumar, A. Govindaraj, and C.N.R. Rao, Chem. Phys. Lett. **307**, 158 (1999).
- [22] Y. Miyamoto, M.L. Cohen, and S.G. Louie, Solid State Commun. **102**, 605 (1997).
- [23] E. Hernández, C. Goze, P. Bernier, and A. Rubio, Appl. Phys. A **68**, 287 (1999).
- [24] J.-Y. Yi and J. Bernholc, Phys. Rev. B **47**, 1708 (1993).
- [25] Nonlocal pseudopotentials are generated for C and N atoms with a 36 Ry energy cutoff for the plane wave expansion of the wavefunctions.
- [26] R. Haydock, V. Heine, and M.J. Kelly, J. Phys. C. **5**, 2845 (1972).
- [27] The tight-binding Hamiltonian is restricted to 2p electrons ( $\pi$  and  $\pi^*$  orbitals only), and the parameters are chosen so as to reproduce the correct band gap for BN and  $\text{BC}_2\text{N}$  nanotubes and the acceptor and donor levels for substitutional C (B or N) atoms in BN-based (C-based) systems [see Ref.12].
- [28] A.Y. Liu and M.L. Cohen, Science **245**, 841 (1989).
- [29] D.M. Teter and R.J. Hemley, Science **271**, 53 (1996).
- [30] E. Hernández, P. Ordejon, I. Boustani, A. Rubio, and J. A. Alonso, J. Chem. Phys. **113**, 3814 (2000).